



HAL
open science

Three-dimensional structural evolution of the cuttlefish *Sepia officinalis* shell from embryo to adult 6 stages

Charles Le Pabic, Julien Derr, Gilles Luquet, Pascal-Jean Lopez, Laure
Bonnaud-Ponticelli

► **To cite this version:**

Charles Le Pabic, Julien Derr, Gilles Luquet, Pascal-Jean Lopez, Laure Bonnaud-Ponticelli. Three-dimensional structural evolution of the cuttlefish *Sepia officinalis* shell from embryo to adult 6 stages. *Journal of the Royal Society Interface*, 2019, 16 (158), pp.20190175. 10.1098/rsif.2019.0175 . hal-02318453

HAL Id: hal-02318453

<https://hal.science/hal-02318453v1>

Submitted on 17 Oct 2019

HAL is a multi-disciplinary open access archive for the deposit and dissemination of scientific research documents, whether they are published or not. The documents may come from teaching and research institutions in France or abroad, or from public or private research centers.

L'archive ouverte pluridisciplinaire **HAL**, est destinée au dépôt et à la diffusion de documents scientifiques de niveau recherche, publiés ou non, émanant des établissements d'enseignement et de recherche français ou étrangers, des laboratoires publics ou privés.

1
2
3
4
5
6
7
8
9
10
11
12
13
14
15
16
17
18
19
20
21

Article type: Full length article

Three-dimensional structural evolution of the cuttlefish *Sepia officinalis* shell from embryo to adult stages.

Charles Le Pabic^a, Julien Derr^b, Gilles Luquet^a, Pascal-Jean Lopez^a, Laure Bonnaud-Ponticelli^{a*}

^aUnité Biologie des organismes et écosystèmes aquatiques (BOREA), Muséum national d'Histoire naturelle, UMR CNRS 7208, Université de Caen Normandie, Sorbonne Université, IRD 207, Université des Antilles, 75005 Paris, France

^bLaboratoire Matière et Systèmes Complexes (MSC), Université Paris Diderot, UMR CNRS 7057, 75205 Paris Cedex 13, France

*Corresponding author. Tel.: + 33 1 40 79 53 48

E-mail address: laure.bonnaud@mnhn.fr (L. Bonnaud-Ponticelli)

Running head: *Sepia* shell 3D-structure

22 Abstract

23 The cuttlefish shell is an internal structure with a composition and general organization unique among
24 molluscs. Its formation and the structure-function relation are explored during *Sepia officinalis*
25 development, using Computerized Axial Tomography Scanning (CAT-scan) 3D analyses coupled to
26 physical measurements and modelling. In addition to the evolution of the overall form, modifications
27 of the internal structure were identified from the last third embryonic stages to adult. Most of these
28 changes can be correlated to life cycle stages and environmental constraints. Protected by the capsule
29 during embryonic life, the first internal chambers are sustained by isolated pillars formed from the
30 dorsal to the ventral septum. After hatching, formation of pillars appears to be a progressive process
31 from isolated points to interconnected pillars forming a wall-delineated labyrinthine structure. We
32 analysed the interpillar space, the connectivity and the tortuosity of the pillar network. The
33 labyrinthine pillar network is complete just prior to the wintering migration, probably to sustain the
34 need to adapt to high pressure and to allow buoyancy regulation. At that time, the connectivity in the
35 labyrinth is compensated by an increase in tortuosity, most probably to reduce liquid diffusion in the
36 shell. Altogether these results suggest adjustment of internal calcified structure development to both
37 external forces and physiological needs.

38

39 Keywords: Cuttlefish; Shell; 3D-Structure; Tomography; Development; Buoyancy

40

41 **1. Introduction**

42 The external calcified shell of molluscs has been selected for its protective functions against predators
43 and/or resistance against stressful physico-chemical factors. The cephalopods are the only molluscs
44 building a chambered shell (phragmocone) used as a buoyant system [1], giving them an adaptive
45 advantage in aquatic environment. Extinct ammonites and present nautiloids show an external
46 chambered shell. During evolution, the external shell has been reduced and internalized in some
47 lineages of cephalopods. As a consequence, behavioural, anatomical and physiological adaptations
48 had to be selected to compensate the loss of the external protective function. In some groups of
49 cephalopods, the internal chambered shell is strongly mineralized with mechanical but also
50 physiological roles as in extinct belemnites, the closest relatives of present lineages, and two present
51 groups of cephalopods: spirulids and sepiids. The sepiid shell, called the cuttlebone, presents
52 numerous differences with that of nautiloids and spirulids. These later organisms build spiral shells
53 with about 30 large chambers, delimited by septa, filled with gas and liquid via a median tubular
54 structure (the siphuncle) passing through the chambers. At the contrary, in sepiids, the shell is flat
55 and formed one hundred of thin chambers separated by septa, all opened posteriorly, where gas/liquid
56 exchanges are regulated through this opened posterior area called siphuncular zone [1,2]. Moreover,
57 each sepiid chamber is supported inside by vertical elements called ‘pillars’, spread over the entire
58 septal surface and forming a complex labyrinthine structure unique in cephalopods, so-called ‘pillar
59 network’ [3,4]. Some hypotheses about spatial organization and organo-mineral formation of this
60 pillar network have been previously proposed for *Sepia* shells [4-9], but with little investigation at
61 the spatial and temporal scales. Yet, such a peculiar structuration should be considered in relation to
62 physiological needs of the organism. Here, we have chosen to study the *Sepia officinalis* shell during
63 its life cycle, from embryo to adult, with a special emphasis on spatio-temporal evolution of the pillar
64 network, *i.e.* inside the same chamber and in different chambers of the same shell. Using
65 Computerized Axial Tomography Scanning (CAT-scan) 3D observations coupled with physical
66 measurements and mathematical analyses, we describe the shell synthesis sequence and the global

67 inside structure of cuttlefish shell, from embryonic to adult stages. Our results, associated with
 68 knowledge about the *S. officinalis* ecology, allow us to link shell structure with cuttlefish life stages
 69 and to hypothesize about the labyrinthine pillar network role in the cuttlefish shell buoyancy function,
 70 an essential prerequisite to further evolutionary studies.

71

72 **2. Materials and Methods**

73 2.1. Research Specimens

74 The lengths, ages and sample keys of the five *S. officinalis* shells used in this study are indicated in
 75 Table 1. All animals come from the English Channel and are at different ontogenic stages. In order
 76 to determine precisely their stage of development, they were reared at the “Centre de Recherches en
 77 Environnement Côtier” (Luc-sur-Mer, France) allowing a day-to-day follow up except for the adult
 78 stage (*i.e.* specimen MNHN IM-2012-13927) that was trawl-fished. Embryonic stages were
 79 determined according to the development table from Lemaire [10]: the shell begins to form at stage
 80 25, when the embryo resembles an adult and the chambers appear progressively until hatching at
 81 stage 30.

82

83 Table 1. Sample keys and age data of *Sepia officinalis* shells used in this study

Sample key	Age	Shell Length (mm)	Shell Width (mm)	Width/Length ratio
MNHN-IM-2012-36001	Embryonic stage 27	3.5	2.1	0.60
MNHN-IM-2012-36006	Embryonic stage 30	6.0	3.5	0.58
MNHN-IM-2012-13923	1 month	11.0	5.7	0.52
MNHN-IM-2012-13925	3 months	33.2	13.0	0.39
MNHN-IM-2012-13927	18 months?	218.4	68.7	0.31

84

85 During egg and juvenile rearing, water parameters were kept at $17 \pm 1^\circ\text{C}$, 32.5 ± 1 psu (salinity) and
 86 $< 0.5 \text{ mg.l}^{-1}$ for ammonia- and nitrite-nitrogen and $< 80 \text{ mg.l}^{-1}$ for nitrate-nitrogen [11]. Juveniles

87 were fed once a day with live brown shrimps *Crangon crangon* during all their maintenance. Before
88 shell removal, cleaning and storage in 70% ethanol, animals (*i.e.* embryo and juveniles) were
89 euthanized by 10% ethanol exposure during 10 min followed by cephalopodium (*i.e.* head, arms and
90 funnel) removal [12,13]. The specimens MNHN IM-2012-36001 and MNHN IM-2012-36006 are
91 both embryonic shells corresponding respectively, to the beginning, stage 27, and to the end, stage
92 30, of the embryonic shell formation. According to the strong influence of food supply and
93 temperature on the *S. officinalis* shell growth [14,15], the choice of the juvenile shells MNHN IM-
94 2012-13923 (1-month old) and MNHN IM-2012-13925 (3-month old) were considered as the best
95 compromise to study shell formation during the juvenile life period. The adult cuttlebone for SEM
96 comes from specimen freshly fished along the English Channel coastline.

97

98 2.2. X-ray tomography

99 For the five *S. officinalis* shells, a high-resolution Computerized Axial Tomography Scanning (CAT-
100 scan) was acquired at the Platform AST-RX of the Museum National d'Histoire Naturelle (MNHN).
101 In order to keep similar resolution in the first built chambers, a second CAT-scan was acquired for
102 the specimen MNHN IM-2012-13925 (3-month old) focusing on the 15 first chambers of this shell.
103 Data relative to this scan are bracketed here below next to the whole shell scan of the same specimen.
104 The scanning parameters were respectively for the specimens IM-2012-36001 (stage 27), IM-2012-
105 36006 (stage 30), MNHN IM-2012-13923 (1 month), MNHN IM-2012-13925 (3 months) and IM-
106 2012-13927 (adult): an effective energy of 70, 70, 65, 55 (68) and 80 kV, a current of 180, 215, 250,
107 310 (275) and 300 mA, a voxel size 2.09, 3.36, 6.17, 18.25 (6.32) and 116.52 μm , and a view number
108 of 2,500, 3,000, 1,800, 1,500 (3,000) and 1,200. Images were reconstructed and exported into 16-bit
109 TIFF stacks using ImageJ 2.0.0 and Avizo Lite 9.0.1 softwares.

110

111 2.3. Scanning Electron Microscopy

112 In order to compare images resulting from CAT-scan and microscopy, small pieces of an adult *S.*
113 *officinalis* cuttlebone (135-mm shell length) were prepared for optical and scanning electron
114 microscopy (SEM) observations. For SEM, cuttlebone pieces were mounted on SEM stubs and
115 covered with a 10-nm gold layer through sputtering using a Jeol FJC-1200 metal coater. SEM
116 observations were performed with a Hitachi SU 3500 microscope using the BSE (backscattered
117 electron) mode.

118

119 2.4. Physical analysis of the inside shell pillar network

120 In order to perform repeatable and comparable height measurements (inside a same shell and between
121 different shells), we set up the following methodology. Along the shell sagittal plan, we measured
122 the greatest chamber height perpendicular to the bottom septa median plan (figure S1). Except for the
123 first synthesized chambers (of each shell), this measure is always located at the front extremity of the
124 top chamber. Height measurements were made using ImageJ 2.0.0 software.

125 Because our observations of the inner parts in studied shells did not underline major structural
126 differences between the same chambers of different shells, we chose the 3-month old shell for the
127 work on the pillar network (*i.e.* connectivity, interpillar space and tortuosity). Each physical analysis
128 has been made on every 3-month shell chambers (*i.e.* from chamber 1, the first one built in embryo
129 to chamber 34, the last chamber formed in the 3-month shell). All image processing was done using
130 the *scikit-image* python package [16].

131 In order to determine if the different inner chamber zones (*i.e.* space zones) are connected together,
132 particularly in chambers with complex pillar network, we used standard image processing techniques
133 [17,18], implemented in the *scikit-image* package [16], which enable to label a binary image by
134 counting the connected regions. From that, we were able to draw a histogram of the size distribution
135 of the different connected regions.

136 To estimate the pillar spacing, for each chamber, we cropped a region representative of the chamber
137 (typically situated at the centre of the chamber) and used directly the cropped image in grayscale. We

138 estimated the interpillar spacing by using a method base on auto-correlation as described in figure
139 S2. To access the typical space between pillars, we performed multiple times 1D cut of the image.
140 For each trial, starting and ending points were randomly picked in the image with the only condition
141 that the length of the cut would be bigger than a minimum value (arbitrarily picked as half the
142 minimum dimension of the cropped image). A grayscale 1D profile was recorded along the cut. These
143 1D profiles exhibited oscillations, but not long enough to efficiently perform Fourier transform.
144 Instead, we chose a similar technique based on auto-correlation (Philippi, personal communication).
145 We computed the autocorrelation of the profile, and as the signal is roughly sinusoidal, the
146 autocorrelation profile presents first a minimum when signals are in opposite phase and then a
147 maximum when they are back in phase. Positions of the first local minimum and first local maximum
148 gave two measurements of the same typical spatial period of the signal. To be sure that our trial is
149 meaningful, we considered the measurement as valid if and only if the relative difference between
150 the two measurements was less than 0.5%. Repeating the trials, we obtained, for each chamber, a
151 distribution of measurements of the spatial period.

152 To describe the pillar network tortuosity, for each chamber, we used the same selection of images as
153 described for pillar spacing measurements. We performed a binarization of the cropped image in
154 grayscale using Otsu's method [19]. Then, we computed the corresponding topological skeleton: a 1-
155 pixel wide skeleton of the object, with the same connectivity as the original object. Applying a generic
156 filter on the skeleton enabled to discriminate between segment pixels, edge pixels or crossing pixels.
157 From there, one can transform the skeleton into a graph structure. For graph structures, classical
158 Dijkstra's algorithm has been used to compute shortest path [20], *i.e.* to go from one point A to one
159 point B. The tortuosity of this path is defined mathematically as the arc/chord ratio: the ratio of the
160 length of the path \widehat{AB} to the Euclidian distance \overline{AB} . The starting points and the ending points are
161 randomly picked in the cropped image (following a uniform distribution). Tortuosity is computed for
162 this path, and the operation is repeated a number of times to get statistics. For each chamber, we
163 performed thousands of trials in order to get a standard error of typically less than one percent. Then,

164 we performed the same analysis in segregating between horizontal and vertical orientation of the
165 paths. We chose the simplest criteria: if the angle between the Euclidian path (starting to ending point)
166 and the horizontal line was more than 45 degrees, we defined it to be vertical, or horizontal if less
167 than 45 degrees.

168 To check the homogeneity of the results among one chamber (which is always bigger than the cropped
169 probe area), we performed the same analysis on chamber 30 by shifting the probe area from -1 to 1
170 time its size.

171

172

173 **3. Results**

174 Cuttlebone grows by ventral accretion of chambers from the posterior to the anterior part of the shell
175 during the whole cuttlefish life. Most of the time, the first synthesized chambers (*i.e.* embryonic) are
176 neither observable nor accessible in adult shell (even young) because of the important growth and
177 calcification of the animal during its life cycle (Table 1).

178

179 3.1. Embryonic stages (*i.e.* 27 and 30)

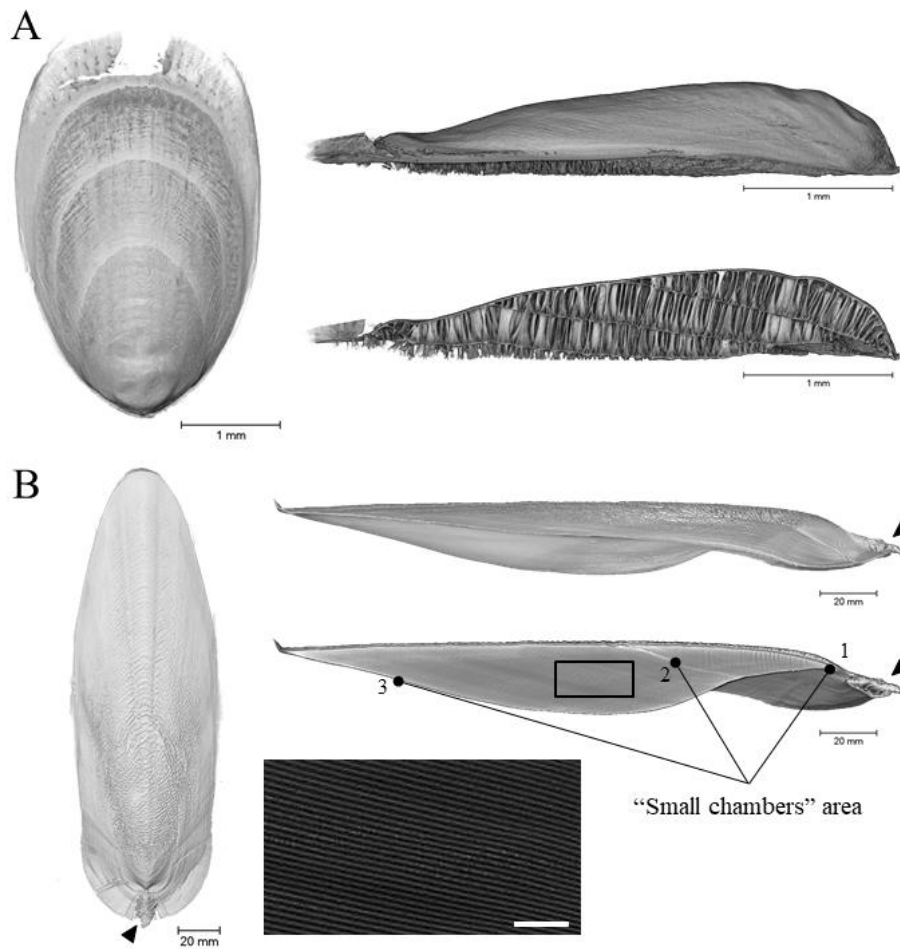
180 The shells from stage 27 and stage 30 embryos are made up of 3 and 6 chambers, respectively (figure
181 1A & figure S3), as previously observed [4-10]. Their heights range from 0.25 to 0.31 mm with a
182 mean chamber height of 0.27 ± 0.02 and 0.28 ± 0.03 mm (mean \pm sd) for stage 27 and stage 30
183 embryo shells, respectively (figure 2).

184

185

186

187

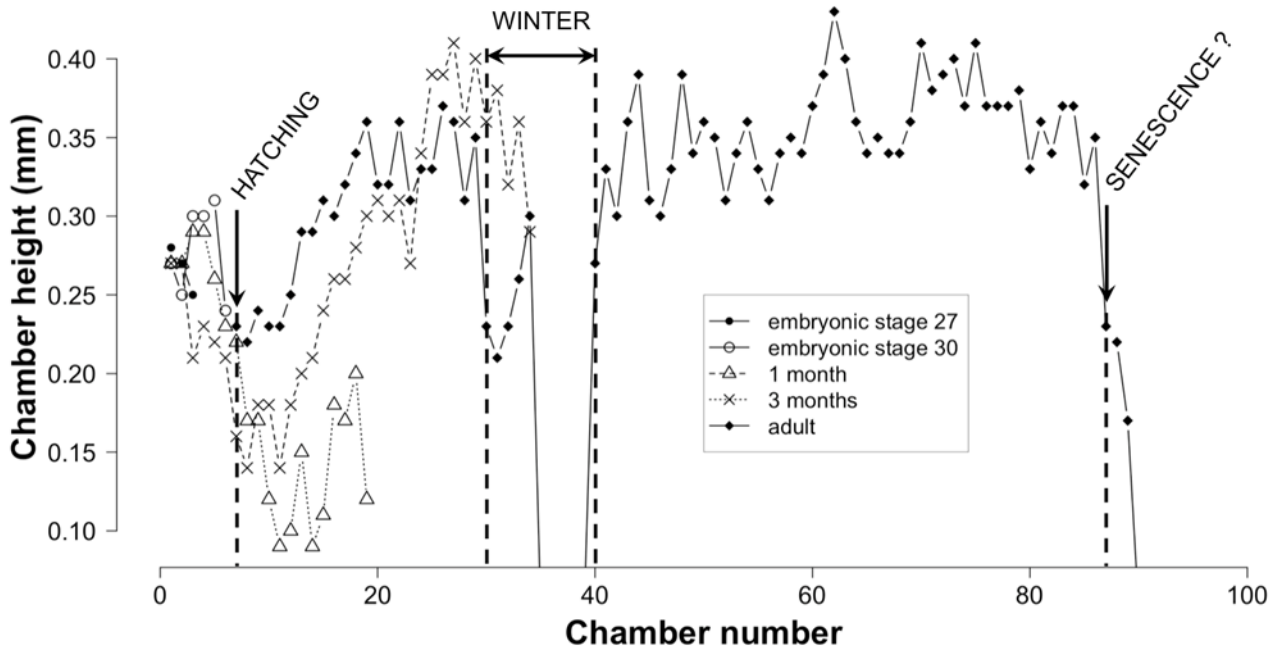


188

189 **Figure 1.** 3D images of A) embryonic stage 27 and B) adult cuttlefish shell. The growth allometry is
 190 clearly visible between embryo and adult. Arrowheads indicate the spine. The three “small chambers”
 191 area indicated on adult shell correspond to chambers too small and/or thin to be precisely counted
 192 and measured. The magnification panel of the adult shell scan highlights the shell septa. Scale bar: 5
 193 mm.

194

195



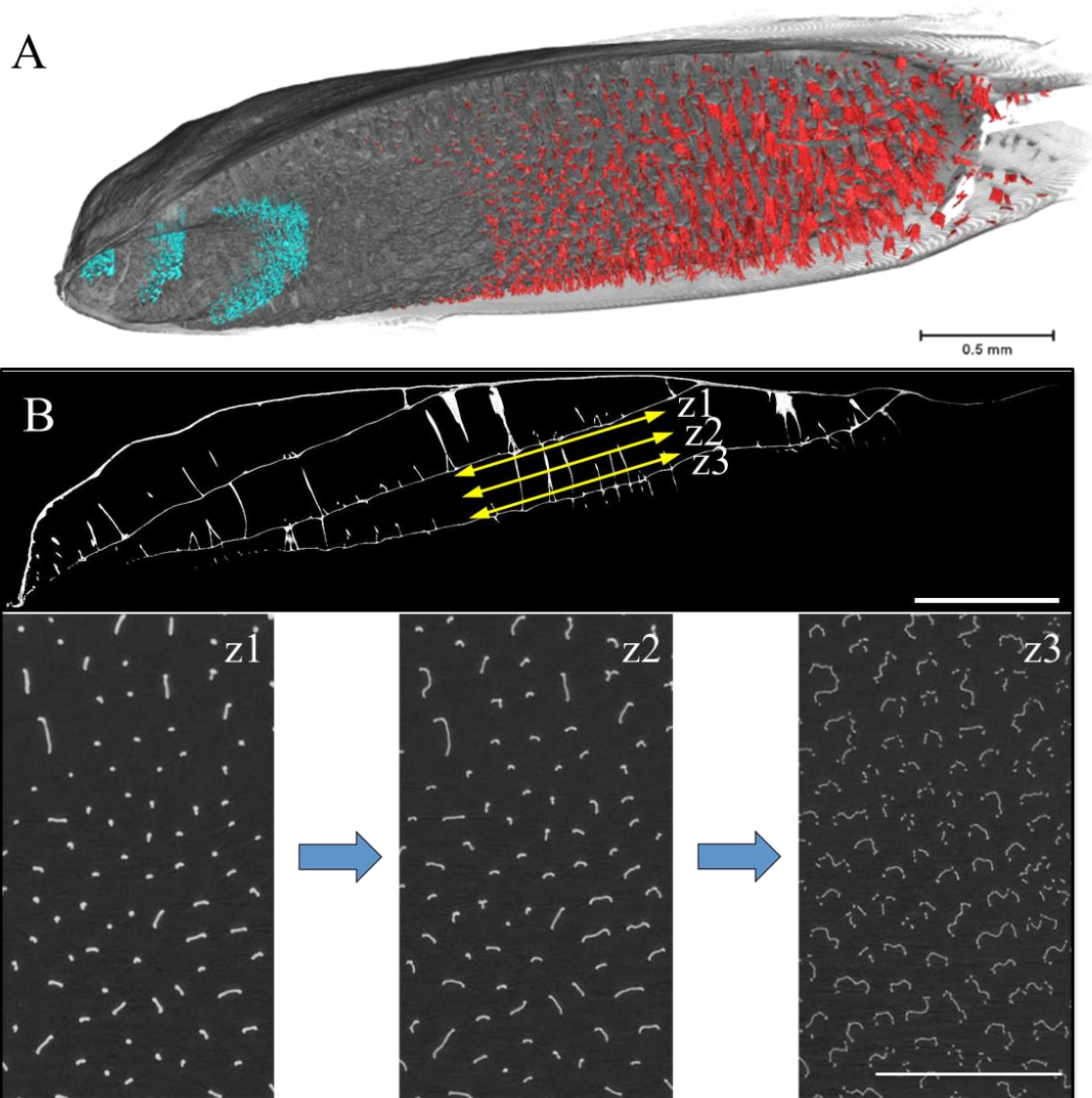
196

197 **Figure 2.** Chamber heights in the different studied shells (embryonic stages 27 and 30, 1-month and
 198 3-month old juveniles, and adult) associated to major events occurring during life cycle.

199

200 In both shells, we observe distinct pillars (*i.e.* disconnected from each other). The pillar shape and
 201 organization are different in the siphuncular area and in the plane-anterior area. In the first one, their
 202 density is higher, and they present in a large majority a straight cylindrical shape with bulging at their
 203 ventral side (figure 3A & figure S4-movie). In the anterior area, their shapes are either cylindrical or
 204 elongated along the sagittal axis (figure 3). From dorsal to ventral septum, most of these pillars widen
 205 to finally form branches with an increase in tortuosity for the elongated pillars (figure 3B). The stage
 206 27 shell X-ray tomography allowed us to observe the beginning of the 4th chamber build up process,
 207 with the dorso-ventral growth of pillars prior to the septa floor formation. We also evidenced that the
 208 pillars are formed progressively from anterior to posterior: there is no pillar building in the same time
 209 on all the chamber surface (figure 3A & figure S4-movie).

210



211

212 **Figure 3.** A) 3D image of embryonic stage 27 shell ventral view with colouring of the two pillar
 213 shapes and organization area (red: “branching” pillars; blue: “siphuncle” pillars), and B) X-ray
 214 tomography pictures of stage 27 shell illustrating the pillar shape evolution. Top picture is a sagittal
 215 plan scan along the three formed chambers with arrows z1, z2, and z3 in chamber 3 localizing (bottom
 216 pictures) the observations made from dorsal to ventral shell side. Scale bars: 0.5 mm.

217

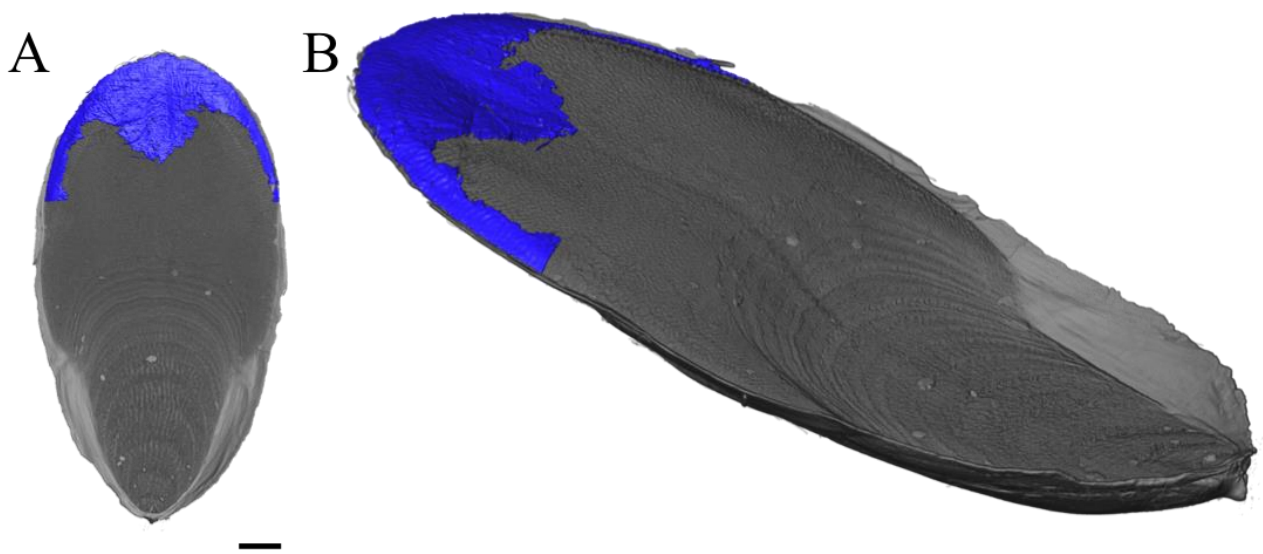
218

219

220 3.2. Juvenile stages (*i.e.* 1- and 3-month old animals)

221 Juvenile shells from 1- and 3-month old cuttlefish reared in controlled conditions are respectively
222 made up of 19 and 34 chambers (figure S3). Whereas absent from embryonic shells, the spine is
223 clearly present in both juvenile shells highlighting the synthesis of this structure after hatching (figure
224 S3, arrowheads). The 1-month old shell scan allowed us to observe the formation of a new septum
225 (figure 4). It appears that this chamber built up step occurs from the front to the back of the shell,
226 similarly to the pillar formation described in section 3.1.

227



228

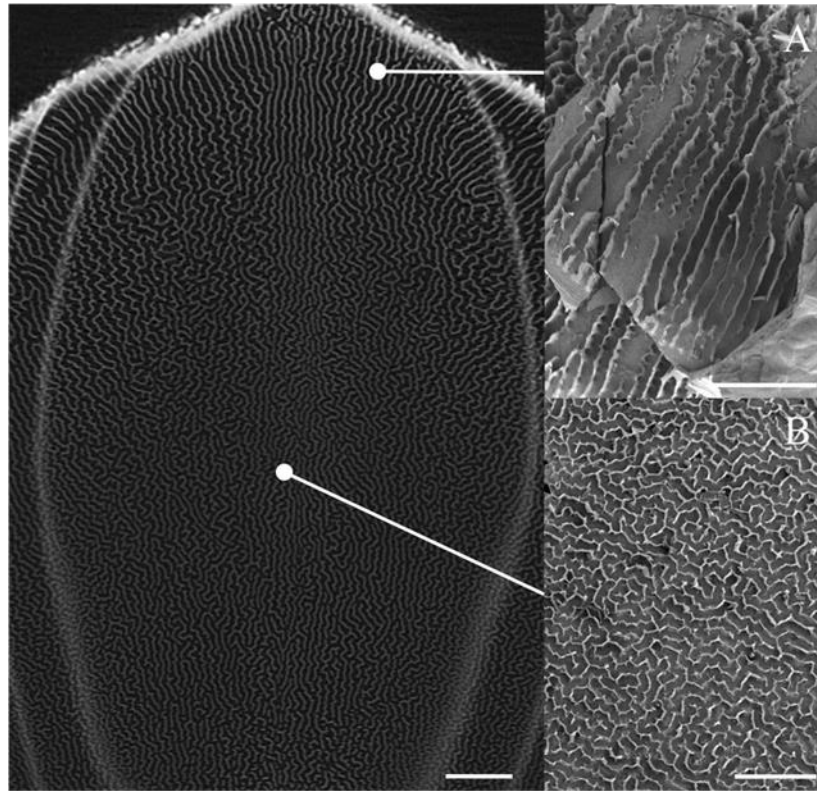
229 **Figure 4.** 3D images of 1-month old cuttlefish shell highlighting in blue the area of the newly septum
230 built from anterior to posterior A) Ventral view (scale bar: 1 mm) and B) Ventro-lateral view.

231

232 The chamber heights range from 0.10 to 0.41 mm with a mean chamber height of 0.18 ± 0.07 and
233 0.27 ± 0.08 mm, for 1- and 3-month old shell, respectively. These important variations (RSD = 39
234 and 30 %, respectively) are due to chamber height decrease (below 0.20 mm) from chambers 8 to 12,
235 observed in both shells (figure 2). Looking at the mineral structures inside of the chamber shell, from
236 the dorsal to the ventral side of the shell, the width of the pillar increases and their tips mainly
237 correspond to tortuous elongated lines in place of the branching described in embryonic chambers.

238 This chamber-to-chamber change results in the progressive linkage of pillars forming a labyrinth
239 network near the 25th shell chamber (figure 5 & figure S5-movie).

240



241

242 **Figure 5.** Labyrinthine structure of the pillar network: Left: X-ray tomography picture highlighting
243 the pillar network organizations (30th chamber of 3-month shell in top view), Right: BSE-SEM
244 images of (A) a linear pillar network configuration (5 kV) found in anterior part and (B) a curved
245 configuration (15 kV) found in the central chamber part. Scale bars: 1 mm.

246

247 3.3. From embryo to adult: the growth of the shell

248 From an external view, the overall main dimensions of the shell increase. During the cuttlefish life
249 cycle, the width/length ratio of the shell is divided by two (0.6 to 0.3; Table 1), with important
250 decrease between embryonic stages and 3-month shell from 0.6 to 0.39. Our data are consistent with
251 those of Sherrard obtained on three adult *S. officinalis* shells coming from Mediterranean Sea
252 (average width/length ratio: 0.36 for an average shell length of 146 mm) [3]. Same author highlighted
253 that such width/length ratio is significantly higher in adult shells coming from *Sepia* species living in

254 shallow area (< 100 m) than those living more in depth (> 100 m), suggesting the shell surface
255 importance to deal with higher pressure. According to this observation, we propose that this change
256 of width/length ratio during the first months of life could be necessary to the *S. officinalis* migration
257 in deeper waters during winter.

258

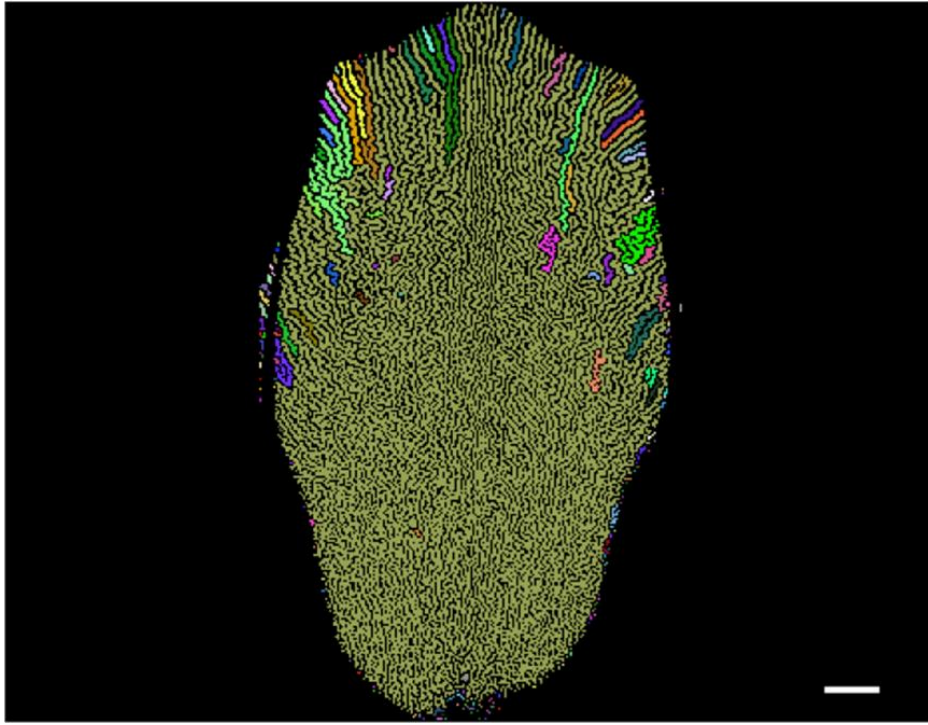
259 3.4. Adult stage

260 The CAT-scan resolution of the image of an adult shell (even if of important size: 218.4 mm; Table
261 1) allowed us to determine that it is made up of more than 100 chambers. Among these chambers, it
262 has been possible to measure 84 chamber heights (figure 2). The heights range from 0.17 to 0.43 mm
263 with a mean chamber height of 0.33 ± 0.05 mm. We observed a progressive increase of the first
264 chamber heights corresponding to the beginning of the juvenile stage (estimated to be from chambers
265 8 to 19; figure 2). The 16 (at least) other chambers were too small and/or thin to be precisely counted
266 and measured (figure 1B). As a whole, three distinct area of these “small chambers” were identified
267 in adult shell (from early to later stages of life): 1) the 6 first chambers (embryonic life), 2) from
268 chambers 35 to 40 (at least), and 3) the 3 last synthesized chambers (at least).

269

270 3.5. Physical measurements and analyses

271 The analysis of the connectivity showed that the pillar network constitutes an almost unique space,
272 whatever its complexity. Indeed, from chambers 15 to 34, we found connection values of the total
273 chambers above 90% (figure 6).

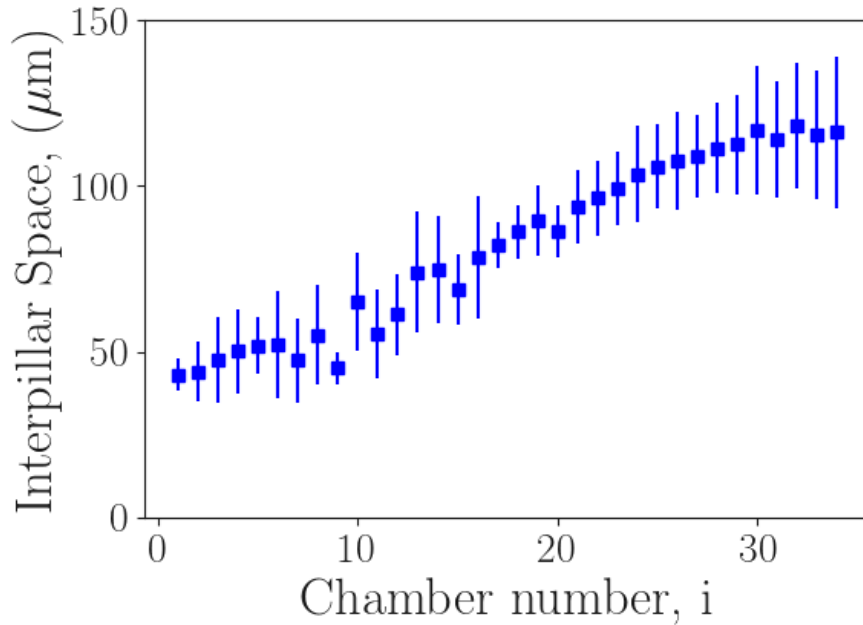


274

275 **Figure 6.** X-ray tomography picture of one of the last chamber (32th chamber) of 3-month shell after
276 connectivity analysis. The different colours represent areas found to be unconnected. Scale bar: 1
277 mm.

278

279 Our analysis of the interpillar space evolution in the 34 first synthesized chambers (*i.e.* in 3-month
280 old shell) highlighted three phases (figure 7).



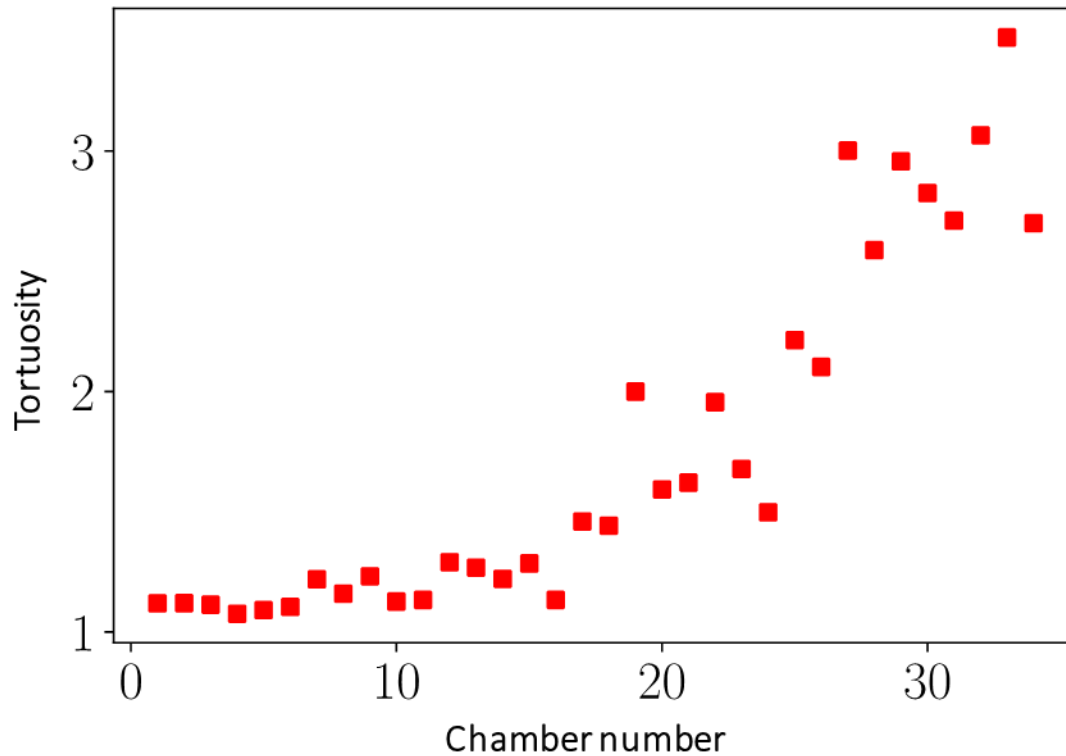
281

282 **Figure 7.** Graph representing the evolution of interpillar space in the different chambers of the 3-
 283 month shell (mean \pm standard deviation, see Materials and Methods).

284

285 Firstly, the values of interpillar space from chamber 1 ($43.0 \pm 4.8 \mu\text{m}$) to chamber 9 ($45.0 \pm 4.9 \mu\text{m}$)
 286 remain stable. Then, interpillar space values increase progressively until chamber 27 (108.8 ± 12.5
 287 μm) to finish by a stable phase from chamber 28 ($111.4 \pm 13.7 \mu\text{m}$) to chamber 34 ($116.3 \pm 22.9 \mu\text{m}$)
 288 with mean values around $114.9 \pm 2.4 \mu\text{m}$. Notably, interpillar spaces and chamber heights appear
 289 positively correlated ($p\text{-value} = 9.68 \times 10^{-10}$; Pearson correlation coefficient = 0.83).

290 The measurements of the tortuosity show three phases as well. From chamber 1 to 16, tortuosity
 291 values are around 1. Then an important increase occurs until chamber 27, before a stabilization of
 292 tortuosity values around 3 (figure 8).



293

294 **Figure 8.** Graph representing the evolution of pillar network tortuosity (arithmetic mean) in the
 295 different chambers of the 3-month shell.

296

297 Then, we performed the same analysis in segregating between horizontal and vertical orientation of
 298 the paths. The vertical paths are mostly parallel to the roughly vertical alignment of the channels
 299 while the horizontal paths are mostly orthogonal to the main orientation of the channels. We chose
 300 the simplest criteria: if the angle between the Euclidian path (starting to ending point) and the
 301 horizontal line was more than 45 degrees, we defined it to be vertical, or horizontal if less than 45
 302 degrees. Following these criteria, we found that horizontal tortuosity increases more than vertical one
 303 during shell building (figure S6). This calculation is congruent with the SEM image showing a linear
 304 pillar network structure in the shell anterior part (figure 5).

305

306

307

308 **4. Discussion**

309 Adult shell CAT-scan opens interesting prospects for the study of cuttlefish shell, and indirectly their
310 development, ecology and evolution. Indeed, it exists more than 100 cuttlefish species having various
311 habitats (*e.g.* depth, temperature) and building shells with important interspecific dimorphism [21].

312 Our three-dimensional observations have evidenced how the cuttlebone is built and, associated with
313 physical measurements, have revealed major changes of the shell inner structure during the first
314 months of life of the cuttlefish.

315 Our results on chamber height measurements highlight some interesting variations consistent with *S.*
316 *officinalis* life stages (figure 2). After hatching, juveniles stay onshore during few months to benefit
317 from coastal prey abundance and rapid growth [22]. During this period (*i.e.* from 8-chamber shell), a
318 decrease of the chamber heights in 1- and 3-month shells from animals cultured in lab is observed
319 until chamber 12. This reduction can be linked with the physiological immaturity of hatchling
320 cuttlefish. Actually, the digestive duct is still immature at least two weeks after hatching and the
321 growth is limited [23,24]. The reduction of the chamber height could help to reduce its metabolic
322 cost during this period, because of the high energy demand needed for other processes such as
323 physiological adaptations to environment [14]. In the shell of adult, grew in the wild, the firstly
324 synthesized post-hatching chambers present heights relatively constant and higher than those made in
325 shells of reared juveniles (1- and 3-month old), which, according to our hypothesis, could be due to
326 a better quality, diversity and a higher quantity of food at hatching. Indeed, the shell growth is known
327 to depend both on the water temperature and food level [25]. After the first weeks post-hatching, the
328 chamber heights (measured in 3-month and adult cuttlebones) increase until chamber 20, when
329 juvenile is mature and initiates its fast growth (figure 2). Then, the chamber heights reach values
330 around 0.35 mm with less variability in both shells, except between the 30th and 40th chambers and
331 after the 86th chamber (adult shell) where two important decreases are observed. This phenomenon
332 has been previously described in cuttlefish from the English Channel as the result of animal wintering
333 conditions [2,26], and firstly linked with slower growth due to colder temperatures and reduced

334 feeding incurred by *Sepia officinalis* during this period of migration [14,15]. In addition, Sherrard
335 associated also this change with depth, highlighting that cuttlebones with low chamber heights are
336 more resistant to pressure [3]. However, the decreases observed in the 3-month old shell, as well as
337 in the last chambers of the adult shell (around the 90th chamber), could also be the sign of the
338 senescence of the animal, due in the first case to rearing conditions, and in the second case to the
339 adult's end of life (cuttlefish are semelparous animals living no longer than 2 years). This smaller
340 size is probably a consequence of the decrease in metabolism and cell activity linked to the feeding
341 decrease of the animals [27].

342 By CAT-scan analysis, we confirmed that pillar growth occurs from dorsal to ventral side as
343 previously described with microscopic observation for this species [4] and for *Sepia esculenta* [6].
344 During this growth, pillar shape changes from a linear proximal basis to a very curved, branched
345 distal (and apical) part. This shape change is more visible in the first formed chambers, those
346 synthesized during embryonic period of life (figure 3) [4]. We also validated that pillars are
347 synthesized from the anterior to the posterior part of each chamber [6], before the building of the
348 chamber floor following the same gradient (figure 3 & figure 4) [3,5,7].

349 In addition, we evidenced a progressive linkage of the chamber pillar network resulting in a complex
350 labyrinthine structure and determined the temporal sequence of this process. Indeed, at the end of the
351 embryo development, in all chambers, the pillars remain isolated (*i.e.* the pillar network does not have
352 a connected structure), whereas around chamber 25 the pillar network appears entirely connected.
353 This stage is estimated to correspond to a juvenile cuttlefish between 1- and 2-month old, *i.e.* few
354 weeks before they realize an autumnal migration offshore to overwintering grounds in the deep
355 central waters of the Channel [22]. As the pillar network constitutes a major innovation in cephalopod
356 shell architecture by its role in avoiding implosion from hydrostatic pressure [3], we propose that the
357 pillar network connection is a major event conferring to *S. officinalis* shell its high compressive
358 strength, making possible migration in deeper areas.

359 Our interpillar space measurements are consistent with partial measurements previously done on *S.*
360 *officinalis* adult shell chambers using SEM [3,28]. Nevertheless as they are the first made on all the
361 chambers from the same cuttlefish shell they are robust and show that there is no high variations
362 between chambers (figure 7). Interestingly, the positive correlation found between this parameter and
363 the chamber height indicates a co-regulation of these structural parameters involved in the cuttlebone
364 porosity [29], but is not consistent with a shell evolution towards a higher compressive strength.
365 However, the evolution of these two parameters (increasing until chamber 20; figure 2 & figure 7)
366 associated with the complete pillar network connection (occurring around chamber 25), suggests that
367 it is during this period that cuttlebone acquires its known mechanical properties of high porosity
368 (93%) [30] and high compressive strength (≥ 15 atm) [31]. Although more CAT-scan analysis have
369 to be done on pillar network at different cuttlefish life stages, our SEM personal observations on
370 different adult cuttlebones suggest that labyrinthine structure is an homogeneous structure between
371 different individuals.

372 Measurements made on the evolution of the pillar network tortuosity highlight an important change
373 in the inner cuttlefish shell structure never shown before (figure 8). Interestingly, there is a continuous
374 process from "dotted" patterns at early stages to "stripes" patterns at later stages until complete inter
375 pillar connection. The general configuration of labyrinth building, whatever the sepiid species,
376 appears biologically controlled, but no mechanism for such a development has been proposed until
377 now.

378 Regarding the role of such a structure, we propose that this structure plays a role in the buoyancy
379 regulation of the shell. Actually, the buoyancy of *S. officinalis* has been extensively described by
380 Denton *et al.* in the 1960s with numerous physiological experimentations [2,32-35]. They have shown
381 that cuttlefish regulates its buoyancy by filling their cuttlebone chambers with various amount of
382 liquid, compressing gas initially inside chambers. The amount of liquid needed to regulate the
383 cuttlefish position in the water column is adjusted by osmotic regulation between liquid inside
384 cuttlebone and blood vessel in direct contact with siphuncular area. Notably, they described the liquid

385 distribution inside the different chambers: the oldest and most posterior chambers are full of liquid,
386 the following chambers contain liquid localized on the siphuncular side, and the last synthesized
387 “large” chambers are full of gas. Authors explain this liquid distribution by the cuttlefish necessity to
388 compensate its anterior gravity centre (with empty shell) to keep horizontal position in water without
389 effort. However, mechanisms regulating such liquid distribution inside chambers have never been
390 proposed. According to our observations, we propose that the labyrinthine pillar network, observed
391 in the central chamber part from chamber 25, allows keeping liquid next to siphuncular opening in
392 order to facilitate its input/output regulation. Actually, when the pillar network tortuosity increases,
393 the fluid speed is expected to decrease. As the labyrinthine pillar network is mainly continuous (figure
394 6), the tortuosity serves to contain (or to limit) the liquid at posterior position whereas the gas is
395 located anteriorly. This hypothesis is consistent with the cuttlefish life cycle, which does not need to
396 compensate great variations of hydrostatic pressure during its coastal life, whereas these variations
397 are stronger after autumnal migration.

398

399 **5. Conclusion**

400 The non-invasive CAT-scan analysis allowed us to describe the inner structural evolution of the
401 cuttlebone during the life cycle of *S. officinalis*. Measurements made on chamber height, interpillar
402 space and pillar network (connection and tortuosity) highlighted important changes during the
403 embryonic and first months of life of the cuttlefish.

404 The whole aspect of this structure looks clearly like typical reaction-diffusion Turing patterns with a
405 "dotted" to "stripes" transition observed during the development. Such kind of transition can be
406 obtained with a morphogen-based process that remains to be characterized.

407 Our observations underline the structural differences of shell chambers synthesized during
408 embryonic, juvenile and adult stage of life. The *S. officinalis* shell seems to reach a mature cuttlebone
409 structure (in terms of pressure resistance and porosity) around 2 months post-hatching. We clearly
410 show that the pillar network, from isolated pillars first synthesized in embryos, finally form, in adult

411 chamber shells, real walls forming a continuous labyrinth within each of the hundred chambers of the
412 cuttlebone ventral part. We proposed that this peculiar structure has been selected as a way to control
413 the liquid circulation and, concomitantly, the gas-liquid rate within the cuttlebone for buoyancy
414 regulation. Associated with the hydrostatic pressure distribution role of pillars, from the last septum
415 to internal septa, we suggest that the synthesis of such cuttlebone pillar network could correspond to
416 a compromise between pressure compressive strength and buoyancy regulation. Finally, our results
417 open interesting prospects to link environment, structure, function and evolution of mineralized shell,
418 particularly unknown in extinct cephalopod species.

419

420 **Data accessibility.** Data from this study are available as electronic supplementary material.

421

422 **Ethics.** Animal protocols were carried out in accordance with European legislation (directive 2010-
423 63-UE and French decret 2013-118).

424

425 **Authors' contributions.** C.L.P. designed & planned the experiment, performed data collection &
426 analysis, as well as manuscript preparation and editing. J.D. designed & planned the mathematical
427 and physical analyses, as well as manuscript editing. G.L. performed data analysis and manuscript
428 editing. P.-J.L. and L.B.-P. wrote the project, supervised the experiments, and assisted with the data
429 interpretation and manuscript editing. All authors gave final approval for publication and agree to be
430 held accountable for the work performed therein.

431

432 **Competing interests.** The authors have no competing interests.

433

434 **Funding.** This work was supported by ATM “Minéral-Vivant” - Museum National d’Histoire
435 Naturelle.

436

437 **Acknowledgements.** CAT-scan was performed at the AST-RX platform of the MNHN with the help
438 of P. Wills, and SEM analysis on the Electronic Microscopy Technical Platform of the MNHN with
439 the help of G. Toutirais. We thank C. Jozet-Alves and the CREC (University of Caen) for providing
440 shells of juveniles, and J-P. Robin for obtaining adult cuttlefish in fish market of Port-en-Bessin-
441 Huppain.

442

443

444

445

446

References

447

1. Denton EJ. 1974 On buoyancy and the lives of modern and fossil cephalopods. *Proc. R. Soc. London. Ser. B.* **185**, 273-299.

448

449

2. Denton EJ, Gilpin-Brown JB. 1961 The buoyancy of the cuttlefish, *Sepia officinalis* (L.). *J. Mar. Biol. Assoc. U.K.* **41**, 319-342.

450

451

3. Sherrard KM. 2000 Cuttlebone morphology limits habitat depth in eleven species of *Sepia* (Cephalopoda: Sepiidae). *Biol. Bull.* **198**, 404-414.

452

453

4. Le Pabic C, Rousseau M, Bonnaud-Ponticelli L, von Boletzky S. 2016 Overview of the shell development of the common cuttlefish *Sepia officinalis* during early-life stages. *Vie Milieu - Life Environ.* **66**, 35-42.

454

455

456

5. Bandel K, von Boletzky S. 1979 A comparative study of the structure, development and morphological relationships of chambered cephalopod shells. *The Veliger* **21**, 313-354.

457

458

6. Tanabe K, Fukuda Y, Ohtsuka Y. 1985 New chamber formation in the cuttlefish *Sepia esculenta* Hoyle. *Venus* **44**, 55-67.

459

460

7. Checa AG, Cartwright JHE, Sánchez-Almazo I, Andrade JP, Ruiz-Raya F. 2015 The cuttlefish *Sepia officinalis* (Sepiidae, Cephalopoda) constructs cuttlebone from a liquid-crystal precursor. *Sci. Rep.* **5**, 1-13. (doi:10.1038/srep11513)

461

462

- 463 8. Čadež V, Škapin SD, Leonardi A, Križaj I, Kazazić S, Salopek-Sondi B, Sondi I. 2017
464 Formation and morphogenesis of a cuttlebone's aragonite biomineral structures for the
465 common cuttlefish (*Sepia officinalis*) on the nanoscale: Revisited. *J. Colloid Interface Sci.*
466 **508**, 95-104.
- 467 9. Le Pabic C, Marie A, Marie B, Percot A, Bonnaud-Ponticelli L, Lopez PJ, Luquet G. 2017
468 First proteomic analyses of the dorsal and ventral parts of the *Sepia officinalis* cuttlebone. *J.*
469 *Proteomics* **150**, 63-73.
- 470 10. Lemaire J. 1970 Table de développement embryonnaire de *Sepia officinalis* L. (Mollusque,
471 Céphalopode). *Bull. Soc. Zool. Fr.* **95**, 773-782.
- 472 11. Oestmann DJ, Scimeca JM, Forsythe J, Hanlon RT, Lee P. 1997 Special considerations for
473 keeping cephalopods in laboratory facilities. *J. Am. Assoc. Lab. Anim. Sci.* **36**, 89-93.
- 474 12. Sykes AV, Baptista FD, Gonçalves RA, Andrade JP. 2012 Directive 2010/63/EU on animal
475 welfare: a review on the existing scientific knowledge and implications in cephalopod
476 aquaculture research. *Rev. Aquac.* **4**, 142-162.
- 477 13. Butler-Struben HM, Brophy SM, Johnson NA, Crook RJ. 2018 *In vivo* recording of neural
478 and behavioral correlates of anesthesia induction, reversal, and euthanasia in cephalopod
479 molluscs. *Front. Physiol.* **9** (109). (doi.org/10.3389/fphys.2018.00109)
- 480 14. von Boletzky S. 1974 Effets de la sous-nutrition prolongée sur le développement de la coquille
481 de *Sepia officinalis* L. (Mollusca, Cephalopoda). *Bull. Soc. Zool. Fr.* **99**, 667-673.
- 482 15. Richard A. 1969 The part played by temperature in the rhythm of formation of markings on the
483 shell of cuttlefish *Sepia officinalis* (Cephalopoda, Mollusca). *Experientia* **25**, 1051-1052.
- 484 16. van der Walt S, Schönberger JL, Nunez-Iglesias J, Boulogne F, Warner JD, Yager N, Guillard
485 E, Yu T, the scikit-image Contributors. 2014 scikit-image: image processing in Python. *PeerJ*
486 **2**, e453. (doi: 10.7717/peerj.453)
- 487 17. Fiorio C, Gustedt J. 1996 Two linear time union-find strategies for image processing. *Theor.*
488 *Comput. Sci.* **154**, 165-181.

- 489 18. Wu K, Otoo E, Shoshani A. 2005 Optimizing connected component labeling algorithms.
490 *Proc. SPIE Conf. Med. Imag.* **5747**, 1965-1976.
- 491 19. Otsu N. A 1979 threshold selection method from gray-level histograms. *IEEE Trans. Syst.*
492 *Man. Cybern.* **9**, 62-66.
- 493 20. Dijkstra EW. 1971 A short introduction to the art of programming. Eindhoven, The
494 Netherlands: Technical University Editor.
- 495 21. Adam W, Rees WJ. 1966 A review of the cephalopod family Sepiidae. London, England:
496 British Museum-Natural History Editor.
- 497 22. Bloor ISM, Attrill MJ, Jackson EL. 2013 A review of the factors influencing spawning, early
498 life stage survival and recruitment variability in the common cuttlefish (*Sepia officinalis*).
499 *Adv. Mar. Biol.* **65**, 1-65.
- 500 23. Yim M, Boucaud-Camou E. 1980 Etude cytologique du développement post-embryonnaire
501 de la glande digestive de *Sepia officinalis* L. (Mollusque Céphalopode). *Arch. Anat. Microsc.*
502 *Morphol. Exp.* **69**, 59-79.
- 503 24. Le Pabic C, Caplat C, Lehodey J-P, Dallas L, Koueta N. 2015 Physiological perturbations in
504 juvenile cuttlefish *Sepia officinalis* induced by subchronic exposure to dissolved zinc. *Mar.*
505 *Pollut. Bull.* **95**, 678-687.
- 506 25. Martínez P, Bettencourt V, Guerra Á, Moltschaniwskyj NA. 2000 How temperature
507 influences muscle and cuttlebone growth in juvenile cuttlefish (*Sepia elliptica*) (Mollusca:
508 Cephalopoda) under conditions of food stress. *Can. J. Zool.* **78**, 1855-1861.
- 509 26. Hewitt RA, Stait B. 1988 Seasonal variation in septal spacing of *Sepia officinalis* and some
510 Ordovician actinocerid nautiloids. *Lethaia* **21**, 383-394.
- 511 27. Boletzky, S. V. (1974). Effets de la sous-nutrition prolongée sur le développement de la
512 coquille de *Sepia officinalis* L.(Mollusca, Cephalopoda). *Bull. Soc. Zool. Fr*, 99(4), 667-673.
- 513 28. Florek M, Fornal E, Gómez-Romero P, Zieba E, Paszkowicz W, Lekki J, Nowak J,
514 Kuczumow A. 2009 Complementary microstructural and chemical analyses of *Sepia*

- 515 *officinalis* endoskeleton. *Mater. Sci. Eng. C* **29**, 1220-1226.
- 516 29. Gutowska MA, Melzner F, Pörtner HO, Meier S. 2010 Cuttlebone calcification increases
517 during exposure to elevated seawater pCO₂ in the cephalopod *Sepia officinalis*. *Mar. Biol.*
518 **157**, 1653-1663.
- 519 30. Birchall JD, Thomas NL. 1983 On the architecture and function of cuttlefish bone. *J. Mater.*
520 *Sci.* **18**, 2081-2086.
- 521 31. Ward PD, von Boletzky S. 1984 Shell implosion depth and implosion morphologies in three
522 species of *Sepia* (Cephalopoda) from the Mediterranean Sea. *J. Mar. Biol. Assoc. UK* **64**, 955-
523 966.
- 524 32. Denton EJ, Gilpin-Brown JB. 1959 Buoyancy of the cuttlefish. *Nature* **184**, 1330-1331.
- 525 33. Denton EJ, Gilpin-Brown JB. 1961 The effect of light on the buoyancy of the cuttlefish. *J.*
526 *Mar. Biol. Assoc. UK* **41**, 343-350.
- 527 34. Denton EJ, Gilpin-Brown JB. 1961 The distribution of gas and liquid within the cuttlebone.
528 *J. Mar. Biol. Assoc. UK* **41**, 365-381.
- 529 35. Denton EJ, Gilpin-Brown JB, Howarth JV. 1961 The osmotic mechanism of the cuttlebone.
530 *J. Mar. Biol. Assoc. UK* **41**, 351-364.

531

532